

Kinetic Analysis for Crystal Growth Rate of NH_4Cl in the $\text{NaCl-MgCl}_2\text{-H}_2\text{O}$ System with a Thermodynamic Approach

Daoguang Wang and Zhibao Li

Key Laboratory of Green Process and Engineering, National Engineering Laboratory for Hydrometallurgical Cleaner Production Technology, Institute of Process Engineering, Chinese Academy of Sciences, Beijing 100190, PR China

DOI 10.1002/aic.12604

Published online March 28, 2011 in Wiley Online Library (wileyonlinelibrary.com).

*A growth kinetic model has been developed from a rigorous thermodynamic perspective to describe the crystal growth rates of NH_4Cl on the basis of the difference of chemical potentials of NH_4Cl at solid–liquid interface in aqueous NH_4Cl , $\text{NH}_4\text{Cl-NaCl}$, and $\text{NH}_4\text{Cl-MgCl}_2$ solutions. The solid–liquid equilibrium and activity coefficient of NH_4Cl are calculated by the newly developed accurate Pitzer model with aid of Aspen PlusTM platform. The predictions of the resulting model are in good agreement with the experimental data published in literature and determined in this work at 283.15–333.15 K within the supersaturation up to 0.1. The kinetic model was subsequently used to analyze the effect of several operation variables, including temperature (283.15–333.15 K), supersaturation (up to 0.1), and NaCl or MgCl_2 concentration ($0\sim 2.5\text{ mol kg}^{-1}$), on the crystal growth rate of NH_4Cl . The crystal growth rate of NH_4Cl , with activation energy of 39 kJ mol^{-1} , is strongly temperature-dependent and increases with increasing temperature in the three systems investigated. The advantage of MgCl_2 over NaCl on the recovery of NH_4Cl is theoretically and experimentally illustrated from the thermodynamic and kinetic perspectives with the aid of the established model. © 2011 American Institute of Chemical Engineers *AIChE J.*, 58: 914–924, 2012*
Keywords: crystallization, kinetic, crystal growth rate, thermodynamic, chemical potential

Introduction

Crystallization is an important solid–liquid separation technique and has been used to separate and purify a variety of materials including inorganic salt and protein, for the chemical, pharmaceutical, and electronic industries.^{1–4} Crystallization of NH_4Cl has been emphasized for several decades since its importance in the manufacturing of soda in the combination process.⁵ In this process, NH_4Cl is recovered by a cooling crystallization followed by a salting-out crystalliza-

tion with the addition of NaCl . Referring to the soda combination process, a new crystallization process to recover crystalline NH_4Cl as saleable product was successfully proposed and underdeveloped in our laboratory with the addition of MgCl_2 to the NH_4Cl -rich solution generated in the process of MgO production.⁶ The new method mainly consists of three crystallization steps: crystallization of ammonium chloride, crystallization of ammonium carnallite, and decomposition of ammonium carnallite. To recover the crystalline ammonium chloride, a series of strategies and operations, including temperature swing and addition of MgCl_2 , are used to carry the feed NH_4Cl -rich solution to the desired crystallization region, where pure solids of the targeted components can be isolated. In consequence, operation

Correspondence concerning this article should be addressed to Z. Li at zhibao.li@mail.ipe.ac.cn.

temperature and solution properties, that is, NaCl or MgCl₂ concentration and supersaturation, play an important role in the crystallization of ammonium chloride in both recovery processes mentioned above. Therefore, the knowledge of the effect of temperature and solutions properties on the crystal growth kinetic of ammonium chloride is of great practical importance for the description of crystallization process and for the practical design and operation of large-scale crystallizers in either the development of new process or improvement of soda combination process.

Experimental investigation of the effect of temperature and solution properties on the crystal growth of NH₄Cl in a particular system is, of course, an option; however, this is a time-consuming enterprise, not to mention that it is not feasible to test all possible combinations of conditions. Development and validation of a kinetic model capable of providing a reliable estimation of crystal growth rate of NH₄Cl in the saturated NH₄-Na-Mg-Cl-H₂O solutions are preferred instead.

Most of the available modeling studies are undertaken on the basis of empirical equations, for example, $G = k\sigma^g$, to correlate experimental data. The driving force (σ) for crystallization is simplified to be the concentration difference $((c-c^*)/c^*)$ between the crystal and the bulk solution.^{7,8} In fact, as Myerson et al.^{9–11} and Mullin and Söhnel¹² have pointed out the fundamental driving force for crystallization is the difference in the chemical potential ($\Delta\mu/RT$) of crystal at the solid–liquid interface. The assumption of using concentration difference instead of the fundamental driving force is inadequate and can lead to significant errors. Subsequently, Mohan and Myerson^{10,11} have successfully established a thermodynamic approach. In this method, an empirical thermodynamic model is used to calculate thermodynamic properties of activity coefficients and chemical potential in supersaturated solutions, to represent the growth kinetic for a number of systems. However, their work focused on the modeling of the growth rates at 298.15 K, with a few attentions given for NH₄Cl-H₂O system, so that the results are not available at either higher or lower temperatures. Moreover, they modeled the growth rate of NH₄Cl in supersaturation range up to 0.25 that corresponds to the growth of the faces of [100], [100i], [110], and [111], as the supersaturation increases.¹³ As the growth rates among different faces are inconsistent,¹⁴ as a consequence, their model shows significant deviation for the prediction of the growth rate of face [1 0 0] in the lower supersaturation range up to 0.06, which is preferred in industrial process (generally $\sigma < 0.1$) to avoid the occurrence of dendrite breeding.¹⁵ Therefore, more modeling studies on the crystal growth kinetics of NH₄Cl to describe the crystal growth rate at low supersaturation are desirable to meet the scaling-up requirements.

The objective of this work is to investigate the effects of temperature and solution properties on the crystal growth rate of NH₄Cl in the NH₄-Na-Mg-Cl-H₂O system by establishing a thermodynamic crystal growth model to be used in the process development and crystallizer design. To be concrete, a kinetic model is first established from a thermodynamic perspective to describe the crystal growth rate of NH₄Cl in the NH₄-Na-Mg-Cl-H₂O system. A newly developed Pitzer model embedded in the commercial Aspen PlusTM software is adopted for the calculation of solubility prediction and activity coefficients. The kinetic model is verified by experimental

data published in literature and determined in this work. Then, the temperature dependence of the crystal growth rate of NH₄Cl in the NH₄-Na-Mg-Cl-H₂O system is investigated by the rigorous, self-consistent theoretical model. The effects of temperature and solution properties, that is, NaCl or MgCl₂ concentration and supersaturation, on the growth rate of NH₄Cl are discussed systematically.

Theoretical Methodology

Driving force for ammonium chloride crystallization

Crystallization reaction of NH₄Cl in the NH₄-Na-Ng-Cl-H₂O system can be described by following equation.



The driving force σ for Eq. 1 is expressed fundamentally by the chemical potential difference at the solid–liquid interface of NH₄Cl species as suggested by Mohan and Myerson^{1,10,11} instead of concentration difference. This can be expressed in dimensionless form as

$$\begin{aligned} \sigma &= \frac{\Delta\mu}{RT} = \left(\frac{\mu_{\text{NH}_4^+}}{RT} + \frac{\mu_{\text{Cl}^-}}{RT} \right) - \left(\frac{\mu_{\text{NH}_4^+}^*}{RT} + \frac{\mu_{\text{Cl}^-}^*}{RT} \right) \\ &= \ln \left(\frac{\gamma_{\pm}^2 m_{\text{NH}_4^+} m_{\text{Cl}^-}}{\gamma_{\pm}^{*2} m_{\text{NH}_4^+}^* m_{\text{Cl}^-}^*} \right) = \ln \left(\frac{\gamma_{\pm}^2 m_{\text{NH}_4^+} m_{\text{Cl}^-}}{K_{\text{SP}}} \right) \end{aligned} \quad (2)$$

where

$$\gamma_{\pm} = (\gamma_{\text{NH}_4^+} \gamma_{\text{Cl}^-})^{1/2} \quad (3)$$

From Eq. 2, it is apparent that the estimation of the fundamental driving force of NH₄Cl in the systems of interest requires the values of solubility of crystalline NH₄Cl, supersaturation, and the corresponding mean activity coefficient of NH₄Cl in the saturated or supersaturated solution. Therefore, the success in modeling crystallization kinetics with the fundamental driving force is strongly dependent on the calculation accuracy of the thermodynamic parameters above.

Solid–liquid equilibrium and activity coefficient calculation

In our previous work, the solid–liquid equilibrium (SLE) in the NH₄Cl-MgCl₂-H₂O system has been successfully represented from 278.15 to 388.15 K by Pitzer model in Aspen PlusTM software. The SLE for the NH₄Cl-NaCl-H₂O system has been successfully described from 273.15 to 373.15 K by Ji et al.¹⁶ with Pitzer model and thus is adopted after verification with the help of Aspen PlusTM platform in this work. Unfortunately, no thermodynamic model has been developed for the calculation of activity coefficient of a supersaturated electrolytic system. In present work, the Pitzer model is also used to calculate the activity coefficients in the supersaturated NH₄-Na-Mg-Cl-H₂O system, because of its successful application in highly concentrated electrolytes (up to 30 m) and elevated temperature (up to 473 K). Activity coefficient expressions have been shown in our previous work for NH₄Cl in the NH₄Cl-MgCl₂-H₂O system. For the NH₄Cl-NaCl-H₂O system, Pitzer¹⁷ described the equation for

Table 1. Pitzer Parameters and Solubility Product Used in the Activity Coefficient Calculation for the NH₄-Na-Mg-Cl-H₂O System

Parameter*	k_1	$10^4 k_2$	k_3	k_4
$\beta_{\text{NH}_4\text{-Cl}}^{(0)16}$	0.0521	26.1316	-436.1570	-2.18043
$\beta_{\text{NH}_4\text{-Cl}}^{(1)16}$	0.1916	52.3542	-212.1680	-2.04936
$C_{\text{NH}_4\text{-Cl}}^{\phi 16}$	-0.0030	-1.45757	32.8062	0.148049
$\beta_{\text{Na-Cl}}^{(0)18}$	0.075359	77.62017	-1123.8799	-5.85883
$\beta_{\text{Na-Cl}}^{(1)18}$	0.277031	98.68215	-1123.6026	-6.429675
$C_{\text{Na-Cl}}^{\phi 18}$	0.001408	1.51976	23.62823	-
$\beta_{\text{Mg-Cl}}^{(0)19}$	0.351083	10.07532	-118.82926	-0.87128
$\beta_{\text{Mg-Cl}}^{(1)19}$	1.651187	-233.59	-102.69541	-5.94902
$C_{\text{Mg-Cl}}^{\phi 19}$	0.006507	12.967	-124.5267	-0.835953
$\theta_{\text{NH}_4\text{-Mg}}^{20}$	-0.044	-	-	-
$\psi_{\text{NH}_4\text{-Mg-Cl}}^{20}$	-0.018	-	-	-
$\theta_{\text{NH}_4\text{-Na}}^{16}$	-0.004519	-	-	-
$\psi_{\text{NH}_4\text{-Na-Cl}}^{16}$	-0.002836	-8.40145	97.961	0.585561
K_{SP}^{16}	2.8491	-8.79	-6620.5112	-15.9329

* $f(T) = k_1 + k_2(T - 298.15) + k_3(\frac{1}{T} - \frac{1}{298.15}) + k_4 \ln(\frac{T}{298.15})$.

activity coefficient of a 1-1 electrolyte NX in a common-ion mixture with a 1-1 electrolyte MX by:

$$\begin{aligned} \ln \gamma_{\text{NX}} = & -\frac{A_\phi}{2} \left[\frac{I^{1/2}}{1 + bI^{1/2}} + \frac{2}{b} \ln(1 + bI^{1/2}) \right] + (1 + y) \\ & \times I[B_{\text{NX}} + IC_{\text{NX}}] + (1 - y)I[B_{\text{MX}} + IC_{\text{MX}} + \theta_{\text{MN}}] + yI^2 \\ & \times (B'_{\text{NX}} + C_{\text{NX}}) + (1 - y)I^2(B'_{\text{MX}} + C_{\text{MX}}) + \frac{1}{2}(1 - y^2)I^2\psi_{\text{MNX}} \end{aligned} \quad (4)$$

where

$$B_{\text{NX}} = \beta_{\text{NX}}^{(0)} + \frac{2\beta_{\text{NX}}^{(1)}}{\alpha^2 I} [1 - (1 + \alpha I^{1/2}) \exp(-\alpha I^{1/2})] \quad (5)$$

$$B'_{\text{NX}} = \frac{2\beta_{\text{NX}}^{(1)}}{\alpha^2 I^2} \left[-1 + \left(1 + \alpha I^{1/2} + \frac{1}{2} \alpha^2 I \right) \exp(-\alpha I^{1/2}) \right] \quad (6)$$

$$C_{\text{NX}} = \frac{C_{\text{NX}}^{\phi}}{2|z_{\text{N}}z_{\text{X}}|^{1/2}} \quad (7)$$

For the system considered in present work, the values of the empirical parameters b and α were taken to be 1.2 and 2.0 (kg/mol)^{-1/2}, respectively.¹⁷ A_ϕ is the Debye-Hückel parameter for the osmotic coefficient, which was obtained from the work of Pitzer.¹⁷ Values of binary Pitzer parameters, that is, $\beta^{(0)}$, $\beta^{(1)}$, and C^ϕ , and mixed parameters, that is, θ and ψ , corresponding to the NH₄Cl-NaCl-H₂O and NH₄Cl-MgCl₂-H₂O systems for activity coefficient calculation are taken or regressed from published literatures (as listed in Table 1).^{16,18-20}

Crystal growth kinetics expression

Generally, crystal growth rate of NH₄Cl is represented by a simple overall growth kinetics expression²¹:

$$G = k\sigma^g \quad (8)$$

From a thermodynamic point of view, the above kinetic expression in terms of the fundamental driving force is

$$G = k' \left(\frac{\Delta\mu}{RT} \right)^{g'} \quad (9)$$

For crystal NH₄Cl, according to the Burton-Cabrera-Frank (BCF) surface diffusion theory,^{11,22} the index g' is equal to 2 at low supersaturation. Then, the growth rate expression of Eq. 9 becomes

$$G = k' \left(\frac{\Delta\mu}{RT} \right)^2 = k' \left(\ln \left(\frac{\gamma_{\pm}^2 m_{\text{NH}_4^+} m_{\text{Cl}^-}}{K_{\text{SP}}} \right) \right)^2 \quad (10)$$

k' is the overall crystal growth rate constant related with temperature and the hydrodynamic state in the solution.^{14,23,24} It can be expressed as a function of temperature as

$$k' = k_0 \exp \left(-\frac{E}{RT} \right) \quad (11)$$

Substituting Eq. 11 into (10), the overall crystal growth rate becomes

$$G = k_0 \exp \left(-\frac{E}{RT} \right) \left(\ln \left(\frac{\gamma_{\pm}^2 m_{\text{NH}_4^+} m_{\text{Cl}^-}}{K_{\text{SP}}} \right) \right)^2 \quad (12)$$

To further explore the temperature and concentration effects on the growth rate of NH₄Cl, the growth rate G is written as

$$G = G_{\text{T}} G_{\text{m}} \quad (13)$$

where

$$G_{\text{T}} = k_0 \exp(-E/RT) \quad (14)$$

Table 2. Experimental Crystal Growth Rate of NH₄Cl in Various Temperatures for the NH₄Cl-NaCl-H₂O and NH₄Cl-MgCl₂-H₂O Systems

<i>T</i> (K)	NH ₄ Cl-NaCl-H ₂ O			NH ₄ Cl-MgCl ₂ -H ₂ O		
	<i>W</i> − <i>W</i> ₀ (g)	<i>G</i> ^{exp} (m s ^{−1})	<i>G</i> ^{cal} (m s ^{−1})	<i>W</i> − <i>W</i> ₀ (g)	<i>G</i> ^{exp} (m s ^{−1})	<i>G</i> ^{cal} (m s ^{−1})
283.15	0.303	6.92 × 10 ^{−8}	8.43 × 10 ^{−8}	1.586	2.79 × 10 ^{−7}	1.72 × 10 ^{−7}
293.15	0.371	8.32 × 10 ^{−8}	9.12 × 10 ^{−8}	2.165	3.51 × 10 ^{−7}	5.09 × 10 ^{−7}
298.15	0.859	1.72 × 10 ^{−7}	9.92 × 10 ^{−8}	2.928	4.33 × 10 ^{−7}	5.34 × 10 ^{−7}
303.15	0.936	1.85 × 10 ^{−7}	1.28 × 10 ^{−7}	3.185	4.59 × 10 ^{−7}	6.35 × 10 ^{−7}
313.15	1.207	2.26 × 10 ^{−7}	1.44 × 10 ^{−7}	3.385	4.78 × 10 ^{−7}	9.03 × 10 ^{−7}
323.15	1.577	2.78 × 10 ^{−7}	1.40 × 10 ^{−7}	4.115	5.42 × 10 ^{−7}	9.43 × 10 ^{−7}
333.15	1.703	2.95 × 10 ^{−7}	1.70 × 10 ^{−7}	4.600	5.82 × 10 ^{−7}	10.4 × 10 ^{−7}

and

$$G_m = \{\ln[(\gamma_{\pm}^2 m_{\text{NH}_4^+} m_{\text{Cl}^-})/K_{\text{SP}}]\}^2. \quad (15)$$

The term *G_T* represents the Arrhenius relationship of the crystal growth rate coefficient.²⁴ The term *G_m* represents the driving force in crystallization by the chemical potential difference of NH₄Cl at the solid–liquid interface.²⁴

Experimental Section

The kinetic model prediction of crystal growth rate of NH₄Cl in the NH₄Cl-H₂O system can be verified by experimental values from Kahlweit.²⁵ However, no experimental data about the growth rate of NH₄Cl in the NH₄Cl-NaCl-H₂O and NH₄Cl-MgCl₂-H₂O systems are available in literatures. The calculations in the NH₄Cl-NaCl-H₂O and NH₄Cl-MgCl₂-H₂O systems are based on the assumption that the activation energy *E* of crystallization and the pre-exponential constant *k*₀ in the NH₄Cl-NaCl-H₂O and NH₄Cl-MgCl₂-H₂O systems are the same as those in the NH₄Cl-H₂O system. New experimental data are measured to verify the reasonableness of the assumption and the reliability of the calculated result of the crystal growth rate of NH₄Cl in the NH₄Cl-NaCl-H₂O and NH₄Cl-MgCl₂-H₂O systems, respectively.

The experiments were carried out in a batch stirred crystallizer (1 L). A certain amount of crystal NaCl or anhydrous MgCl₂ was added to the saturated solution (containing 500 g water) of NH₄Cl at a given temperature to prepare supersaturated solution with the concentration of NaCl or MgCl₂ of 0.08 mol kg^{−1}. At the same time, 1.000 g (*W*₀) of sieved seed crystals of NH₄Cl (0.2~0.25 mm) was added in the solution with stirring speed of 300 rpm to avoid the primary and second nucleation. The temperature was kept constant for about 5 min (*t*), and then the crystals were filtrated, dried, and weighted (*W*). The composition of the crystals was confirmed by the X-ray diffraction (XRD) method. The experimental crystal growth rate of NH₄Cl in the NH₄Cl-NaCl-H₂O and NH₄Cl-MgCl₂-H₂O systems at different temperatures was subsequently calculated by Eq. 16¹⁴ and listed in Table 2.

$$G^{\text{exp}} = 4^{1/3} \cdot \frac{L - L_0}{t} \quad (16)$$

where *L* is the final diameter of the crystals and is calculated by¹⁴

$$L = \left(\frac{W}{W_0}\right)^{1/3} L_0 \quad (17)$$

Results and Discussion

SLE in the NH₄-Na-Mg-Cl-H₂O system: Model verification and comparison

The accuracy of Pitzer model in prediction of SLE in NH₄Cl-MgCl₂-H₂O system has been illustrated in our previous work⁶ and is not demonstrated again in the present work. A comparison of experimental data^{26,27} with the prediction from the Pitzer model embedded in Aspen PlusTM platform by use of parameters taken from Ji et al.¹⁶ is shown in Figure 1 for the SLE in the NH₄Cl-NaCl-H₂O system at 273.15, 323.15, and 373.15 K. It is clear that the calculated values are good in agreement with experimental data, especially in the crystallization region of NH₄Cl.

To appreciate the effect of temperature and NaCl or MgCl₂ on the crystallization of NH₄Cl thermodynamically, Figure 2 exhibits the SLE in the NH₄Cl-NaCl-H₂O and NH₄Cl-MgCl₂-H₂O systems at 283.15 and 333.15 K.²⁷ It is shown that the solubilities of NH₄Cl increase with increasing temperature both in NH₄Cl-NaCl-H₂O and NH₄Cl-MgCl₂-H₂O systems. It indicates that a lower temperature is preferred to obtain a higher yield of NH₄Cl. This is one of the main reasons why

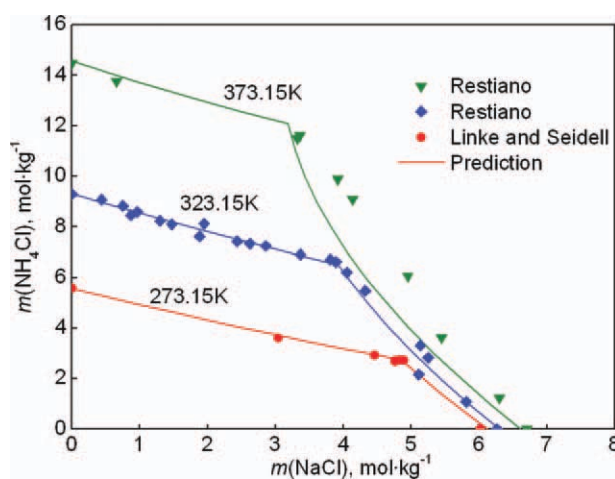


Figure 1. Solid–liquid equilibrium in the ternary NH₄Cl-NaCl-H₂O system at 273.15, 323.15, and 373.15 K.

[Color figure can be viewed in the online issue, which is available at www.interscience.wiley.com.]

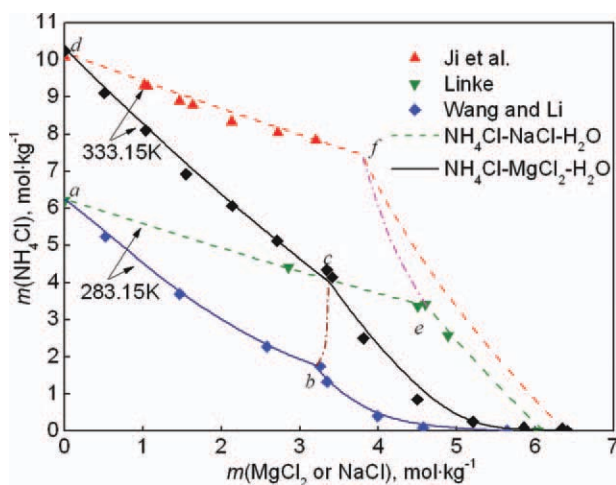


Figure 2. Solid-liquid equilibrium in the ternary NH_4Cl - NaCl - H_2O and NH_4Cl - MgCl_2 - H_2O systems at 283.15 and 333.15 K.

[Color figure can be viewed in the online issue, which is available at wileyonlinelibrary.com.]

the recovery of NH_4Cl in the soda production is operated at low temperature about 280~288 K, meaning high energy-consuming. It is also observed in Figure 2 that the solubility of NH_4Cl is much smaller with addition of MgCl_2 than that with addition of the same molality of NaCl at a certain temperature. This is due to the stronger common ion effect of MgCl_2 because it yields two chloride ions instead of one from NaCl in an aqueous solution. Therefore, a desirable yield of NH_4Cl may be achieved even at a higher temperature with aid of MgCl_2 , as described by the line cd (for NH_4Cl - MgCl_2 - H_2O at 333.15 K) and ae (for NH_4Cl - NaCl - H_2O at 283.15 K).

Growth kinetic model of NH_4Cl : Parameterization and verification

After verifying the thermodynamic model, it is known that the values of model parameters, k_0 and E , should be

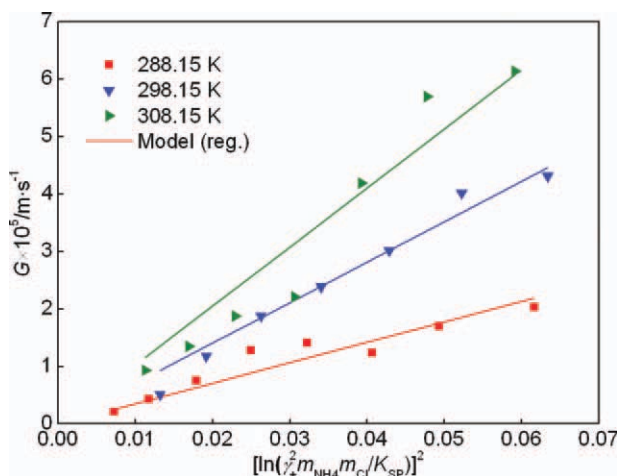


Figure 3. Growth rate vs. $[\ln(\gamma^2 \pm m_{\text{NH}_4} + m_{\text{Cl}})]^2$ for NH_4Cl at 288.15, 298.15, and 308.15 K.

[Color figure can be viewed in the online issue, which is available at wileyonlinelibrary.com.]

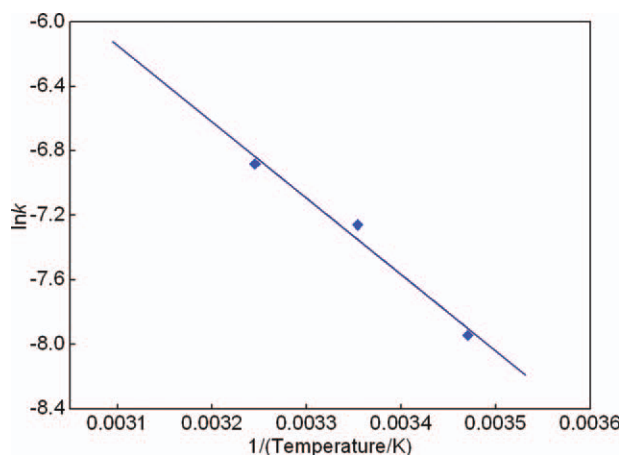


Figure 4. $\ln k'$ vs. $1/T$ for crystal growth rate of NH_4Cl .

[Color figure can be viewed in the online issue, which is available at wileyonlinelibrary.com.]

known before the prediction of crystal growth rate of NH_4Cl in the NH_4 - Na - Mg - Cl - H_2O system. In the present work, the kinetic parameters (growth rate constants) corresponding to Eqs. 8–12, that is, k (or k'), k_0 , and E , were determined by linear regression analysis. The kinetic parameter of k' was correlated on the basis of thermodynamic supersaturation ($\Delta\mu/RT$) calculated by Pitzer activity coefficient model with parameters listed in Table 1. The valid range of supersaturation, σ , corresponds to that of the experimental data for growth rate of NH_4Cl [1 0 0] at 288.15, 298.15, and 308.15 K from Kahlweit.²⁵ As shown in Figure 3, it is observed that the thermodynamic model expression, Eq. 10, well represents the growth kinetics of ammonium chloride at the range of supersaturation and temperature of interest. Values of k' at 288.15, 298.15, and 308.15 K were subsequently obtained and demonstrated in Figure 4. These calculated results were then subjected to regression analysis in the logarithm form of Eq. 11 to obtain the values of k_0 and E . The values of determined k_0 , E , and correlated results are listed in Table 3. It is shown that the activation energy, E , with value of 39.3351 kJ mol^{-1} is typically illustrated by an integration controlled process for the crystal growth rate of NH_4Cl .¹⁴

Following the determination of the model parameters, the verification of the kinetic model was carried out. Figure 5 shows the growth rate as a function of supercooling for ammonium chloride saturated solution at 318.15 and 333.15 K. The experimental values (dot) from Kahlweit²⁵ and Blackmore et al.²⁸ correspond a thermodynamic supersaturation up to 0.1 or more. The experimental data from Blackmore et al. for the model verification was mere one point because their other values at much higher supersaturation are far outside

Table 3. Correlated Activation Energy E and Pre-exponential Factor k_0 from Experimental Results by Kahlweit²⁵

E (kJ mol^{-1})	k_0 (m s^{-1})	R^2	s
39.3351	5006.5380	0.9574	0.01081

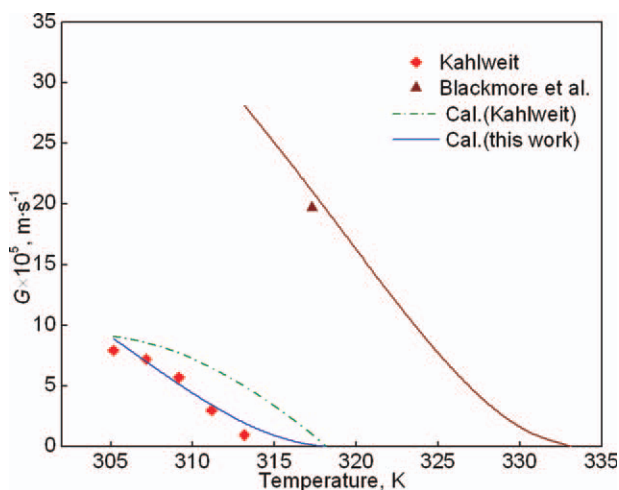


Figure 5. Growth rate of NH_4Cl with increasing supercooling (Saturation temperature 318.15 and 333.15 K).

[Color figure can be viewed in the online issue, which is available at wileyonlinelibrary.com.]

of practical application range. It can be observed from the Figure that predictions of the present model are in good agreement with experimental values. However, the Kahlweit's model²⁵ prediction seems deviated largely from his experimental values. This mainly results from the exclusion of the activity coefficient of NH_4Cl in his model.

The kinetic model was further verified by crystal growth rate data of NH_4Cl in NH_4Cl - NaCl - H_2O and NH_4Cl - MgCl_2 - H_2O systems. The experimental results listed in Table 2 show the crystal growth rate increases with increasing temperatures from 283.15 to 333.15 K by the addition of certain amount of NaCl or MgCl_2 in NH_4Cl - H_2O system. In addition, both the growth rate and the yield of NH_4Cl are higher in aqueous MgCl_2 - NH_4Cl - H_2O system than those in aqueous NaCl - NH_4Cl - H_2O system. The growth rates of NH_4Cl calculated with the developed kinetic model by use of an average supersaturation are also listed Table 2. It seems that the predictions are accordance with experimental results. These results prove the reasonable assumption and the reliability of the calculated results for NaCl - NH_4Cl - H_2O and MgCl_2 - NH_4Cl - H_2O systems.

The SEM images of the crystalline NH_4Cl from aqueous NaCl - NH_4Cl - H_2O and MgCl_2 - NH_4Cl - H_2O solutions are shown in Figures 6b and c, respectively. It is observed that both the produced crystals with addition of NaCl or MgCl_2 exhibit a typical shape similar with the seeded crystals (Figure 6a). Figure 7 shows the XRD patterns of the produced crystals from aqueous NaCl - NH_4Cl - H_2O and MgCl_2 - NH_4Cl - H_2O solutions. It seems that the crystals are pure NH_4Cl , which implies that NaCl and MgCl_2 have been dissolved completely under the experimental conditions. Additionally, the XRD patterns of formed crystals are good in accordance with the standard diffractions (ICDD-00-001-1043). This suggests that high quality of the pure NH_4Cl crystal can be produced effectively from aqueous NaCl - NH_4Cl - H_2O , as well as MgCl_2 - NH_4Cl - H_2O solutions by the described experimental method.

Growth kinetic analysis for NH_4Cl in aqueous $\text{NH}_4\text{Na-Mg-Cl-H}_2\text{O}$ solution

Having established the growth kinetic model, the effects of temperature and solution properties on the growth rate of crystal NH_4Cl can be analyzed by Eq. 12 for aqueous NH_4Cl - H_2O , NH_4Cl - NaCl - H_2O , and NH_4Cl - MgCl_2 - H_2O systems.

Effect of Temperature on the Growth Rate of NH_4Cl in $\text{NH}_4\text{Cl-H}_2\text{O}$ System. Figure 8 shows the temperature effect on the crystal growth rate at different supersaturation ($\Delta m_{\text{NH}_4} = m_{\text{NH}_4} - m^*$) in $\text{NH}_4\text{Cl-H}_2\text{O}$ system calculated by Eq. 12. It is clear that the crystal growth rate increases with increasing temperature at a certain supersaturation and that the increment is enlarged at higher temperature. For example, the growth rate increases from $1.37 \times 10^{-6} \text{ m s}^{-1}$ at 283.15 K to $7.07 \times 10^{-6} \text{ m s}^{-1}$ at 333.15 K at $\Delta m(\text{NH}_4) = 0.2 \text{ mol kg}^{-1}$, indicating a strong temperature dependence. It also can be observed that the crystal growth rate increases with increasing supersaturation at the same temperature.

Figure 9 shows the temperature effect on the Arrhenius coefficient term, G_T , and the driving force term, G_m , of the crystal growth rate. It is observed that the $G_m(\text{NH}_4)$ decreases as the temperature increasing. This can be explained by its definition of Eq. 15. The value of $(\gamma_{\pm}^2 m_{\text{NH}_4^+} m_{\text{Cl}^-})/K_{\text{SP}}$ in the expression for G_m is always more than 1. As the increasing of temperature, the solubility of NH_4Cl in the aqueous solution and the solubility product (K_{SP}) increase, which leads to the decrease of $(\gamma_{\pm}^2 m_{\text{NH}_4^+} m_{\text{Cl}^-})/K_{\text{SP}}$ approaching to unit. It is also

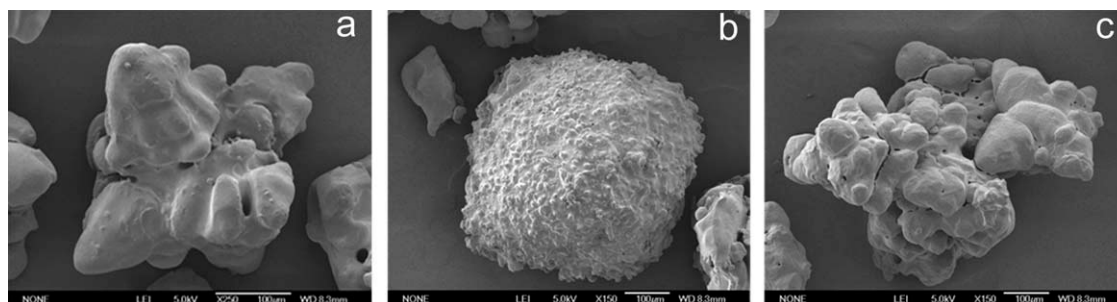


Figure 6. SEM morphologies of crystals of NH_4Cl .

(a) Seeded crystals; (b) prepared crystals in NH_4Cl - NaCl - H_2O system at 303.15 K; (c) prepared crystals in NH_4Cl - MgCl_2 - H_2O system at 303.15 K.

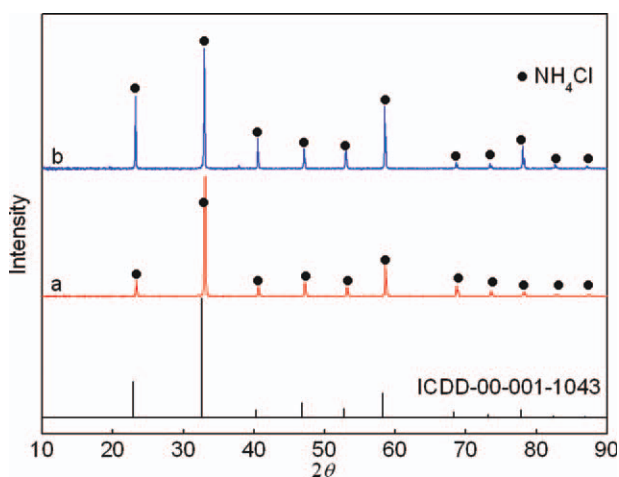


Figure 7. XRD patterns of prepared crystals of NH_4Cl from different systems at 303.15 K.

(a) NH_4Cl - NaCl - H_2O ; (b) NH_4Cl - MgCl_2 - H_2O . [Color figure can be viewed in the online issue, which is available at wileyonlinelibrary.com.]

noted that G_T increases as the increasing of temperature. In the temperature range investigated, G_T seems to be the dominant factor for the growth rate of NH_4Cl crystals, because its behavior minors the curve sharp of growth rate shown in Figure 8. It further indicates that the temperature dependence of growth rate of NH_4Cl is strong and rules out the diffusion of solute as rate-determining step.²⁵

Effect of Temperature on the Growth Rate of NH_4Cl in NH_4Cl - NaCl - H_2O Solution. It is well known that NH_4Cl is recovered from NH_4Cl -rich solutions in the soda production by the addition of NaCl due to the common-ion effect. In this case, the solution becomes an aqueous multiple-electrolyte system. The complicated solution may cause the complexity of the temperature effect on the growth rate of NH_4Cl . Thus, to appreciate the temperature effect on the crystal growth rate of NH_4Cl in the NH_4Cl - NaCl - H_2O system, the kinetic model

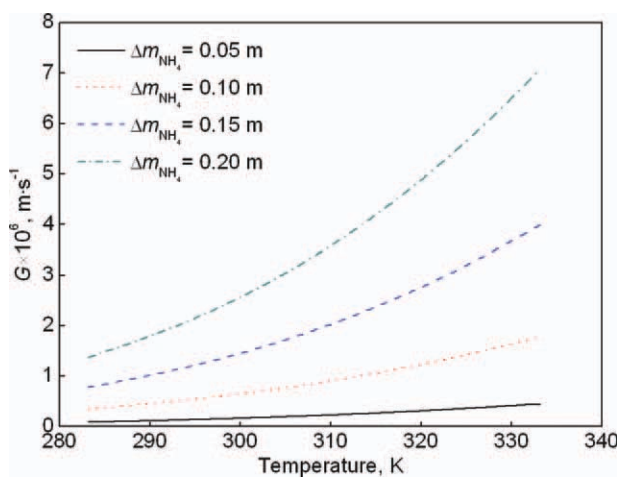


Figure 8. Temperature effect on the crystal growth rate of NH_4Cl in aqueous NH_4Cl solution.

[Color figure can be viewed in the online issue, which is available at wileyonlinelibrary.com.]

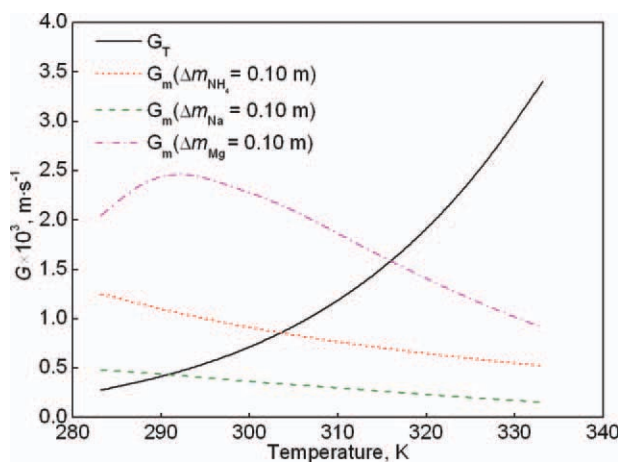


Figure 9. Effects of terms G_T and G_m on the crystal growth rate in the NH_4Cl supersaturation solution.

[Color figure can be viewed in the online issue, which is available at wileyonlinelibrary.com.]

(Eq. 12) is used to investigate the crystal growth rate of NH_4Cl in saturated NH_4Cl solution with addition of NaCl at various temperatures ranging from 283.15 to 333.15 K. It is assumed that the activation energy E of crystallization and the pre-exponential constant k_0 in the Eq. 12 are not affected with presence of NaCl , and thus are the same as those listed in Table 3 for the NH_4Cl - H_2O system. The calculated results are shown in Figure 10. It can be derived that the crystal growth rate of NH_4Cl increases with increasing dosage of NaCl . At a certain dosage of NaCl , the crystal growth rate seems to increase with increasing temperature by a constant increment, for instance, the growth rate increases from $5.32 \times 10^{-7} \text{ m s}^{-1}$ at 283.15 K to $2.08 \times 10^{-6} \text{ m s}^{-1}$ at 333.15 K with $\Delta m(\text{Na}) = 0.2 \text{ mol kg}^{-1}$. The temperature effect on the $G_m(\text{Na})$ is also shown in Figure 9. It is noted that the $G_m(\text{Na})$ decreases as the temperature increases and are in accordance with $G_m(\text{NH}_4)$. The less values of $G_m(\text{Na})$ than $G_m(\text{NH}_4)$

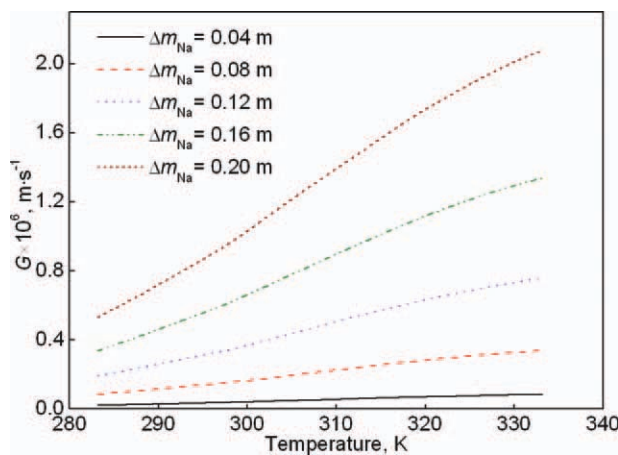


Figure 10. Temperature effect on the crystal growth rate of NH_4Cl in aqueous NH_4Cl - NaCl solution.

[Color figure can be viewed in the online issue, which is available at wileyonlinelibrary.com.]

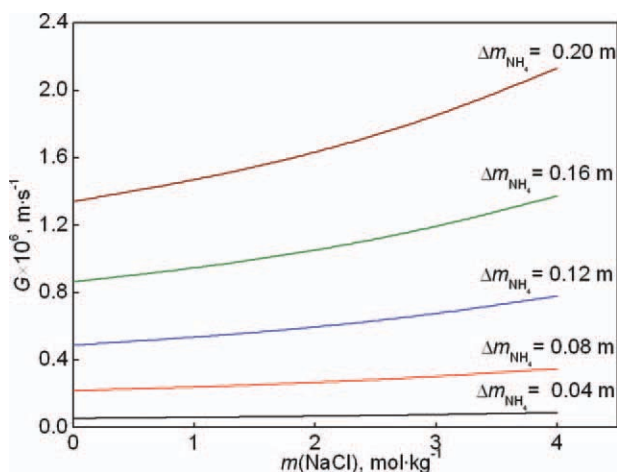


Figure 11. Effect of NaCl concentration on the crystal growth rate in of NH_4Cl aqueous NH_4Cl -NaCl solution in the cooling case at 288.15 K.

[Color figure can be viewed in the online issue, which is available at wileyonlinelibrary.com.]

result from the weaker common effect of NaCl. This may explain why the growth rate at a certain dosage of NaCl and temperature seems to be less than that of the same $\Delta m(\text{NH}_4)$ as shown in Figure 8.

Effect of NaCl Concentration on the Growth Rate of NH_4Cl in NH_4Cl -NaCl- H_2O Solution. In the soda manufacture process, NH_4Cl is recovered consecutively by cooling and salting-out crystallizations. In these two crystallization operations, the supersaturations are generated in different types. The supersaturation in cooling crystallization is obtained by temperature decrease, whereas in salting-out crystallization it is generated by the common ionic effect with addition of NaCl. At this point, the effects of NaCl concentration on the crystal growth rate of NH_4Cl in saturated

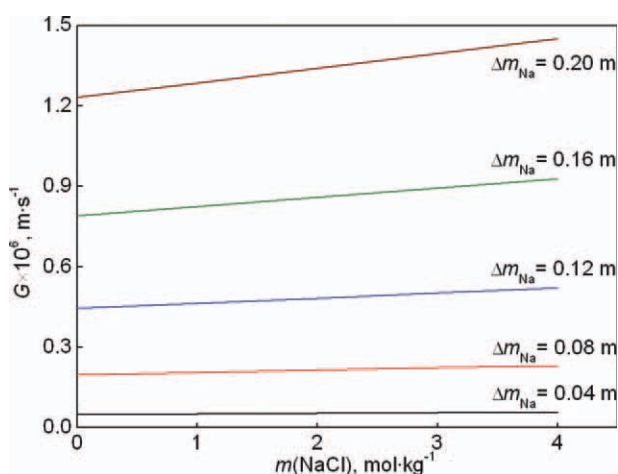


Figure 12. Effect of NaCl concentration on the crystal growth rate of NH_4Cl in aqueous NH_4Cl -NaCl solution in the salting-out case at 283.15 K.

[Color figure can be viewed in the online issue, which is available at wileyonlinelibrary.com.]

NH_4Cl solution (mother liquor) are investigated in cooling and salting-out crystallizations, respectively.

Figure 11 shows the effect of NaCl concentration on the growth rate of NH_4Cl in the case of cooling crystallization with supersaturation in Δm_{NH_4} at 288.15 K. It is clear that the crystal growth rate linearly increases with increasing concentration of NaCl at the same supersaturation of Δm_{NH_4} in solution, which means that a higher concentration of NaCl facilitates the growth of NH_4Cl in a cooling operation.

Figure 12 shows the effect of NaCl concentration on the growth rate of NH_4Cl in the case of salting-out crystallization with the addition of NaCl (Δm_{Na}) at 283.15 K. It is noted that the crystal growth rate of NH_4Cl seems to be affected slightly by the concentration of NaCl with adding the same amount of Δm_{Na} in solution. This means that the NH_4Cl crystal steadily grows with the increase of NaCl concentration in a salting-out operation.

Effect of Temperature on the Growth Rate of NH_4Cl in NH_4Cl - MgCl_2 - H_2O Solution. The temperature effect on the crystal growth rate of NH_4Cl in saturated NH_4Cl solution with addition of MgCl_2 is also investigated with the help of Eq. 12. It is still assumed that the activation energy E of crystallization and the pre-exponential constant k_0 are not affected with presence of MgCl_2 . The calculated results are shown in Figure 13. It is observed that the crystal growth rate of NH_4Cl increases with increasing dosage of MgCl_2 . At a certain dosage of MgCl_2 , the crystal growth rate also increases with increasing temperature, as it is noticed that the growth rate increases from 3.08×10^{-6} to 1.12×10^{-5} m s^{-1} at temperature range 283.15–333.15 K with $\Delta m(\text{Mg}) = 0.2 \text{ mol kg}^{-1}$. However, the increment is reduced at higher temperature. This indicates the stronger temperature effect on the growth rate of NH_4Cl in MgCl_2 - NH_4Cl - H_2O system at the lower temperature range. This is also in accordance with the $G_m(\text{Mg})$ behavior as shown in Figure 9. In the Figure, it is described that $G_m(\text{Mg})$ increases initially with the increase of temperature, passes a maximum at around 293.15 K and then decreases. The maximum of

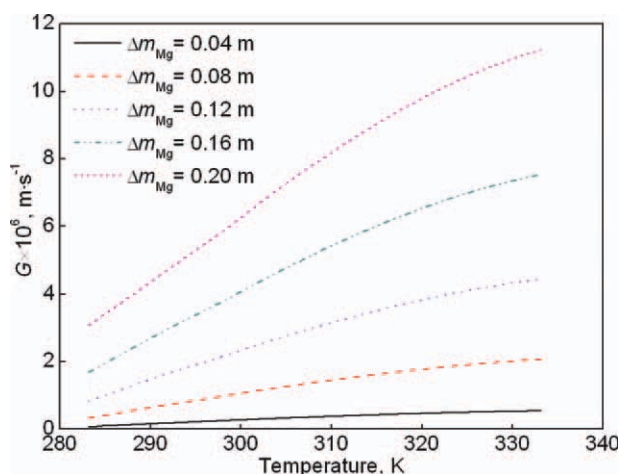


Figure 13. Temperature effect on the crystal growth rate of NH_4Cl in aqueous NH_4Cl - MgCl_2 solution.

[Color figure can be viewed in the online issue, which is available at wileyonlinelibrary.com.]

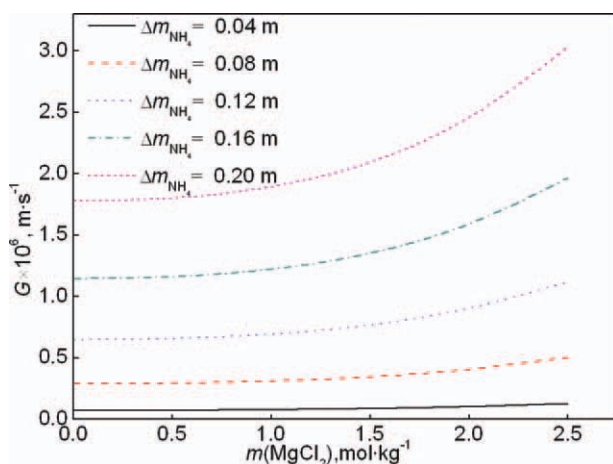


Figure 14. Effect of MgCl_2 concentration on the crystal growth rate in of NH_4Cl aqueous NH_4Cl - MgCl_2 solution in the cooling case at 298.15 K.

[Color figure can be viewed in the online issue, which is available at wileyonlinelibrary.com.]

$G_m(\text{Mg})$ results from the increase of $(\gamma_{\pm}^2 m_{\text{NH}_4^+} m_{\text{Cl}^-})/K_{\text{SP}}$ below 293.15K on the basis of the calculation of supersaturation in chemical potential difference.

Effect of MgCl_2 Concentration on the Growth Rate of NH_4Cl in NH_4Cl - MgCl_2 - H_2O Solution. Similar with the recovery of NH_4Cl in the soda process, the recovery of NH_4Cl in MgO production process is also composed by the two consecutive cooling and salting-out operations.⁶ In the case of cooling crystallization, as shown in Figure 14, the crystal growth rate increases with increasing concentration of MgCl_2 at the same supersaturation of Δm_{NH_4} . Further, the increment is gradually magnified as increasing

concentration of MgCl_2 , suggesting that the presence of MgCl_2 facilitates the growth of NH_4Cl .

In the case of salting-out crystallization, the effect of MgCl_2 concentration on the growth rate of NH_4Cl at 298.15 K is presented in Figure 15. It is shown that the crystal growth rate decreases and then increases with increasing concentration of MgCl_2 by adding the same amount of Δm_{Mg} in solution. This phenomenon can be explained by Figures 14 and 16. Figure 16 describes the effects of MgCl_2 concentration on the precipitated amount of NH_4Cl with the addition of Δm_{Mg} . It can be observed that the precipitated amount of NH_4Cl linearly decreases with increasing MgCl_2 concentration by addition of the same amount of MgCl_2 . It is indicated that the obtained real supersaturation Δm_{NH_4} is lower at higher MgCl_2 concentration range with the addition of a certain dosage of MgCl_2 (Δm_{Mg}). Meanwhile, Figure 14 demonstrates that the crystal growth rate of NH_4Cl increases fast with increasing MgCl_2 concentration at a certain supersaturation of Δm_{NH_4} . As a consequence, a maximum growth rate is obtained in the moderate MgCl_2 concentration.

Comparison of the Effect of NaCl and MgCl_2 on the Crystal Growth Rate of NH_4Cl . It is interesting that how much the dosage of MgCl_2 or NaCl ($\Delta m_{\text{MgCl}_2} = \Delta m_{\text{Mg}}$) should be added to the saturated NH_4Cl solution to reach the same crystal growth rate as that in the single NH_4Cl - H_2O system with supersaturation of Δm_{NH_4} . To solve this problem, following method is developed by combining the growth rate equations both in the NH_4Cl - MgCl_2 - H_2O (3) and NH_4Cl - H_2O systems (1). Now that $G_3(\Delta m_{\text{Mg}}) = G_1(\Delta m_{\text{NH}_4})$, following equation can be derived from Eq. 13.

$$G_{3T}G_{3m}(\Delta m_{\text{Mg}}) = G_{1T}G_{1m}(\Delta m_{\text{NH}_4}). \quad (18)$$

At the same temperature, $G_{1T} = G_{3T}$. Thus,

$$G_{3m}(\Delta m_{\text{Mg}}) = G_{1m}(\Delta m_{\text{NH}_4}) \quad (19)$$

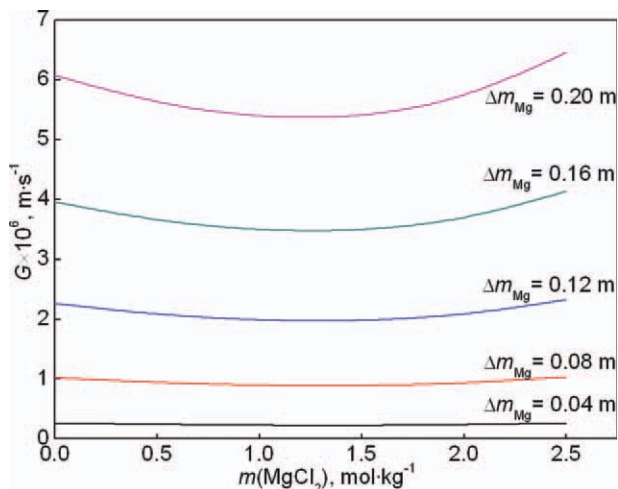


Figure 15. Effect of MgCl_2 concentration on the crystal growth rate of NH_4Cl in aqueous NH_4Cl - MgCl_2 solution in the salting-out case at 298.15 K.

[Color figure can be viewed in the online issue, which is available at wileyonlinelibrary.com.]

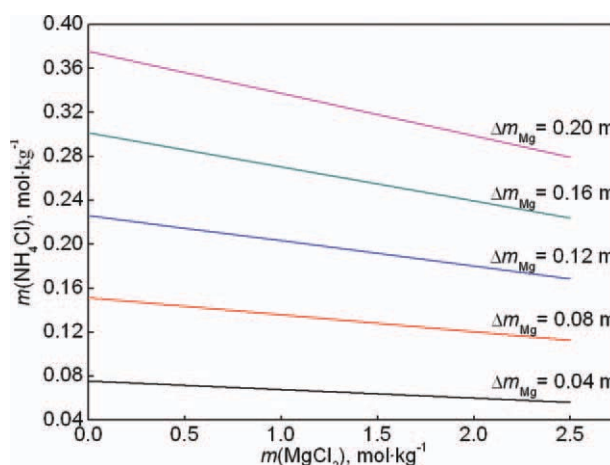


Figure 16. Effect of MgCl_2 concentration on the precipitated amount of NH_4Cl in aqueous NH_4Cl - MgCl_2 solution in the salting-out case at 298.15 K.

[Color figure can be viewed in the online issue, which is available at wileyonlinelibrary.com.]

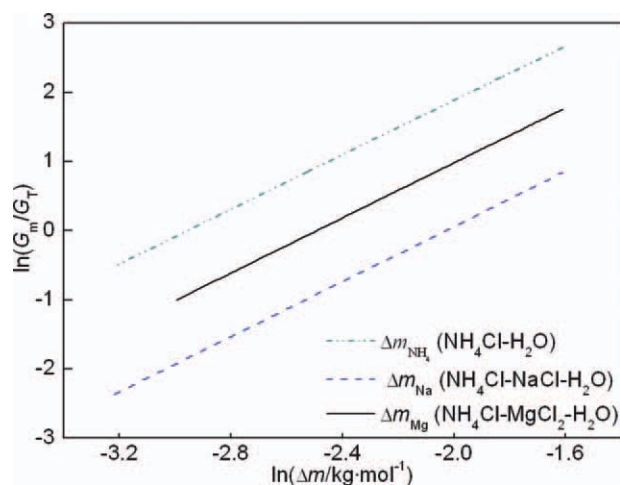


Figure 17. Logarithm of G_m/G_T as a function of logarithm of Δm at 298.15 K.

[Color figure can be viewed in the online issue, which is available at wileyonlinelibrary.com.]

Subsequently, G_T and G_m are calculated at various temperatures and supersaturation by Eqs. 14 and 15, respectively. Further, the relationships among G_T , G_m , supersaturation (Δm), and temperature are investigated. As shown in Figure 17, it is interesting that the value of $\ln(G_m/G_T)$ follows a linear relation as Eq. 20 with $\ln(\Delta m)$ at low supersaturation ($\Delta m < 0.2 \text{ mol kg}^{-1}$) both for Δm_{Mg} and Δm_{NH_4} in the $\text{NH}_4\text{Cl-MgCl}_2\text{-H}_2\text{O}$ and $\text{NH}_4\text{Cl-H}_2\text{O}$ systems at a certain temperature from 283.15 to 333.15 K.

$$\ln(G_m/G_T) = a \ln(\Delta m) + b. \quad (20)$$

The slopes and intercepts of the line for $\ln(G_m/G_T)$ vs. $\ln(\Delta m)$ are calculated at different temperatures and tabulated in Table 4. Following equation will be obtained by combining the Eqs. 18–20.

$$\Delta m_{Mg} = \exp((a_1 \ln(m_{NH_4}) + b_1 - b_2)/a_2). \quad (21)$$

The dosage of MgCl_2 (Δm_{Mg}) added to the saturated $\text{NH}_4\text{Cl-H}_2\text{O}$ system at different temperatures can be calcu-

Table 4. Parameters Fitted for Eq. 20 in the $\text{NH}_4\text{Cl-H}_2\text{O}$, $\text{NH}_4\text{Cl-NaCl-H}_2\text{O}$, and $\text{NH}_4\text{Cl-MgCl}_2\text{-H}_2\text{O}$ Systems

T (K)	NH ₄ Cl-H ₂ O (1)		NH ₄ Cl-NaCl-H ₂ O (2)		NH ₄ Cl-MgCl ₂ -H ₂ O (3)	
	a	b	a	b	a	b
283.15	1.9762	6.0557	1.9942	5.1407	2.2796	7.2654
288.15	1.9769	5.6699	1.9958	4.7895	2.1162	6.7531
293.15	1.9787	5.2978	1.9939	4.4294	2.0193	6.2748
298.15	1.9801	4.9376	1.9917	4.0452	1.9685	5.8211
303.15	1.9801	4.5879	1.9940	3.7044	1.9403	5.4281
308.15	1.9809	4.2495	2.0115	3.3848	1.9228	5.0228
313.15	1.9822	3.9215	1.9837	2.9664	1.9114	4.6200
318.15	1.9824	3.6020	1.9840	2.6028	1.9036	4.2234
323.15	1.9836	3.2919	1.9987	2.2579	1.8973	3.8249
328.15	1.9830	2.9886	1.9863	1.8602	1.8921	3.4258
333.15	1.9845	2.6942	1.9901	1.4881	1.8869	3.0243

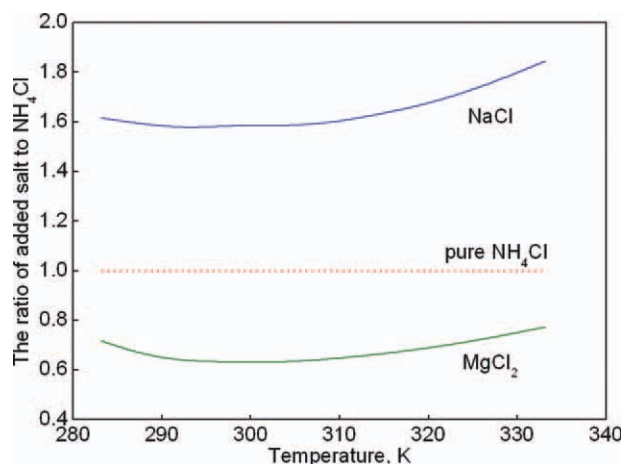


Figure 18. Temperature effect on the ratio of added MgCl_2 to NH_4Cl in saturated NH_4Cl solution at the same crystal growth rate.

[Color figure can be viewed in the online issue, which is available at wileyonlinelibrary.com.]

lated by Eq. 21 with corresponding parameters listed in Table 4. It is found that Δm_{Mg} increases linearly with increasing Δm_{NH_4} in the investigated supersaturation range at each temperature but with different slopes. The effect of temperature on the slopes ($\Delta m_{Mg}/\Delta m_{NH_4}$) is shown in Figure 18. It is observed that the ratio of Δm_{Mg} to Δm_{NH_4} decreases first and then increases with increasing temperature, and the minimum ratio is found at around 298.15 K. This phenomenon can be explained from the behavior of G_m curve, which exhibits a maximum at around 298.15 K as shown in Figure 9. The ratio of Δm_{Mg} to Δm_{NH_4} ranging from 0.6305 to 0.7734 means that a certain crystal growth rate will be obtained with less amount of MgCl_2 than that of NH_4Cl .

Figure 18 also exhibits the effect of temperature on the slopes ($\Delta m_{Na}/\Delta m_{NH_4}$) in the $\text{NH}_4\text{Cl-NaCl-H}_2\text{O}$ system. The relationship of Eq. 20 above also exists with the addition of NaCl (Figure 17). It seems that from Figure 18 the dosage of NaCl added to saturated NH_4Cl solution is about two times of that of MgCl_2 to achieve the same crystal growth rate.

Conclusions

The effects of temperature and solution properties, that is, supersaturation and NaCl/MgCl_2 concentration, on the crystal growth rate of NH_4Cl in aqueous NH_4Cl , $\text{NH}_4\text{Cl-NaCl}$ and $\text{NH}_4\text{Cl-MgCl}_2$ solutions are analyzed by a well-established growth kinetic model developed from thermodynamic perspective on the basis of the difference of chemical potentials of NH_4Cl at solid–liquid interface. The crystal growth rate of NH_4Cl , with activation energy of 39 kJ mol^{-1} , is strongly temperature-dependent and increases with increasing temperature at 283.15 to 333.15 K in supersaturation range up to 0.1 for the three systems of interest in present work. In the case of cooling crystallization, the increment of NaCl or MgCl_2 concentration enhances the growth rate of NH_4Cl in the $\text{NH}_4\text{Cl-NaCl-H}_2\text{O}$ and $\text{NH}_4\text{Cl-MgCl}_2\text{-H}_2\text{O}$ systems. In the salting-out crystallization, the crystal growth rate of NH_4Cl affects slightly by NaCl concentration in the $\text{NH}_4\text{Cl-}$

NaCl-H₂O system, whereas the crystal growth rate decreases and then increases with increasing MgCl₂ concentration in the NH₄Cl-MgCl₂-H₂O system with addition of same amount of MgCl₂. In addition, the dosage of NaCl added to saturated NH₄Cl solution should be two times the addition of MgCl₂ to achieve the same crystal growth rate, and it is shown that MgCl₂ is thermodynamically and kinetically preferred for the recovery of NH₄Cl.

Acknowledgments

The authors gratefully acknowledge the financial support of National Natural Science Foundation of China (Grant No. 21076212, 21076213) and National Basic Research Program of China (973 Program, 2007CB613501, 2009CB219904).

Notation

a = ionic activity product on the basis of molality
 E = activity energy of crystallization (kJ mol⁻¹)
 G = growth rate (m s⁻¹)
 g = growth order
 k, k' = overall growth rate coefficient
 k_0 = pre-exponential constant (m s⁻¹)
 K_{SP} = solubility product
 L = the final crystals size (m)
 L_0 = the initial crystals size (m)
 m = concentration on the basis of molality (mol kg⁻¹)
 R = universal gas constant (J mol⁻¹ K⁻¹)
 t = the residence time (s)
 T = temperature (K)
 W = the final weight of crystals (kg)
 W_0 = the initial weight of crystals (kg)

Greek Letters

γ = activity coefficient
 $\Delta\mu$ = change in chemical potential
 σ = relative supersaturation

Superscripts

* = saturated condition

Literature Cited

- Mullin JW. *Crystallization*, 4th ed. London: Butterworth-Heinemann, 2001.
- Myerson AS. *Handbook of Industrial Crystallization*, 2nd ed. Oxford: Butterworth-Heinemann, 2001.
- Inada T, Modak PR. Growth control of ice crystals by poly (vinyl alcohol) and antifreeze protein in ice slurries. *Chem Eng Sci*. 2006;61:3149–3158.
- Wang XJ, Ching CB. A systematic approach for preferential crystallization of 4-hydroxy-2-pyrrolidone: thermodynamics, kinetics, optimal operation and in-situ monitoring aspects. *Chem Eng Sci*. 2006;61:2406–2417.
- Hou TP. *Soda Engineering*, 1st ed. Beijing: Chemical Engineering Press, 1959.
- Wang DG, Li ZB. Modeling solid-liquid equilibrium of NH₄Cl-MgCl₂-H₂O system and its application to recovery of NH₄Cl in MgO production. *AIChE J*. In press.
- Kumar KV. Regression analysis for the two-step growth kinetics of crystals in pure solutions. *Ind Eng Chem Res*. 2009;48:7852–7859.
- Tai CY, Chang MC, Wu CK, Lin YC. Interpretation of calcite growth data using the two-step crystal growth model. *Chem Eng Sci*. 2006;61:5346–5354.
- Kim S, Myerson AS. Metastable solution thermodynamic properties and crystal growth kinetics. *Ind Eng Chem Res*. 1996;35:1078–1084.
- Mohan R. Crystallization from solution: methods for the study of solubility, kinetics and phase transitions. Ph.D. Thesis. Polytechnic University, Brooklyn, NY, 2001.
- Mohan R, Myerson AS. Growth kinetics: a thermodynamic approach. *Chem Eng Sci*. 2002;57:4277–4285.
- Mullin JW, Söhnel O. Expressions of supersaturation in crystallization studies. *Chem Eng Sci*. 1977;32:683–686.
- Chan SK, Reimer HH, Kahlweit M. On the stationary growth shapes of NH₄Cl dendrites. *J Cryst Growth*. 1976;32:303–315.
- Garside J, Mersmann A, Nyvlt J. *Measurement of Crystal Growth and Nucleation Rates*, 2nd ed. Rugby: IChemE, 2002.
- Mersmann A, Bartosch K. How to predict the metastable zone. *J Cryst Growth*. 1998;183:240–250.
- Ji XY, Lu XH, Zhang LZ, Bao NZ, Wang YR, Shi J, Benjamin CYL. A further study of solid-liquid equilibrium for the NaCl-NH₄Cl-H₂O system. *Chem Eng Sci*. 2000;55:4993–5001.
- Pitzer KS. *Activity Coefficients in Electrolyte Solution*, 2nd ed. Boston: CRC Press, 1991.
- Pitzer KS, Peiper JC, Busey RH. Thermodynamic properties of aqueous sodium chloride solutions. *J Phys Chem Ref Data*. 1984;13:1–102.
- Pabalan RT, Pitzer KS. Thermodynamics of concentrated electrolyte mixtures and the prediction of mineral solubilities to high temperatures for mixtures in the system Na-K-Mg-Cl-SO₄-OH-H₂O. *Geochim Cosmochim Acta*. 1987;51:2429–2443.
- Balarew Chr, Christov Chr, Valyashko V, Petrenko S. Thermodynamics of formation of carnallite type double salts. *J Solution Chem*. 1993;22:173–181.
- Tavare NS. *Industrial Crystallization: Process Simulation Analysis and Design*, 1st ed. New York: Plenum Press, 1995.
- Burton WK, Cabrera N, Frank FC. The growth of crystals and the equilibrium structure of their surface. *Philos Trans Royal Soc London A*. 1951;243:299–358.
- Wu JF, Tai CY, Yang WK, Leu LP. Temperature effects on the crystallization kinetics of size-dependent systems in a continuous mixed-suspension mixed-product removal crystallizer. *Ind Eng Chem Res*. 1991;30:2226–2233.
- Cheng FQ, Bai Y, Liu C, Lu XH, Dong C. Thermodynamic analysis of temperature dependence of the crystal growth rate of potassium sulfate. *Ind Eng Chem Res*. 2006;45:6266–6271.
- Kahlweit M. On the dendritic growth of NH₄Cl crystals from aqueous solution. *J Cryst Growth*. 1970;6:125–129.
- Restiano S, 1938. *Solubilities of Inorganic and Organic Compounds*, 1st ed. Oxford: Pergamon Press, 1979; Cited by Silcock HL.
- Linke WF, Seidell A. *Solubilities of Inorganic and Metalorganic Compounds*, 4th ed. Washington: American Chemical Society, 1965.
- Blackmore KA, Beatty KM, Hui MJ, Jackson KA. Growth behavior of NH₄Cl-H₂O mixtures. *J Cryst Growth*. 1997;174:76–81.

Manuscript received Nov. 25, 2010, and revision received Feb. 17, 2011.